Analogy between one-dimensional chain models and graphene

A. Matulis[a)]
Departement Fysica, Universiteit Antwerpen Groenenborgerlaan 171, B-2020 Antwerpen, Belgium
Semiconductor Physics Institute, Goštauto 11, LT-01108 Vilnius, Lithuania

F. M. Peeters[b)]
Departement Fysica, Universiteit Antwerpen Groenenborgerlaan 171, B-2020 Antwerpen, Belgium

(Received 10 August 2008; accepted 10 April 2009)

The electron and hole spectrum in single and bilayer graphene is derived from known one-dimensional models, and the relation between the spectrum and symmetry of the lattice is shown. © *2009 American Association of Physics Teachers.*
[DOI: 10.1119/1.3127143]

I. INTRODUCTION

Over the last 30 years, there has been much interest in exotic allotropic phases of carbon, for example, C_{60} carbon molecules[1] and carbon nanotubes.[2] Both can be considered as rolled up single layers of graphite. Recently, a single layer of graphite, called *graphene*, has been produced experimentally.[3–5] This ideal two-dimensional system immediately created a large interest in the study of its electron and hole spectra.[6] The electronic spectrum of graphene[7] is shown in Fig. 1 and is a complicated surface indicating the electron energy dependence on its wave vector (or quasi-momentum) $\mathbf{k}=\{k_x,k_y\}$.

At zero temperature, the lower half of this energy band is filled with electrons up to the Fermi surface E_F, as shown in Fig. 1 by the horizontal plane. When the temperature increases, some of the electrons obtain additional energy, leaving holes under the Fermi surface. The energy band shown in Fig. 1 is about 20 eV wide, corresponding to a temperature of 200,000 K. Thus, room temperature, 300 K, is very low compared to this band width. Consequently, these electrons and holes (the low energy excitations) remain close to the Fermi surface. For this reason, it is not necessary to take the entire complicated energy band into account. Only small regions around the K points are of importance. One of them is circled in Fig. 1 and shown separately in Fig. 2(a).

The motion of electrons and holes in graphene in the two cones [see Fig. 2(a)] touching each other by their sharp tops is described by the Schrödinger equation

$$i\hbar\frac{\partial}{\partial t}\Psi(\mathbf{r},t)=H\Psi(\mathbf{r},t), \tag{1}$$

where the Hamiltonian is given by a 2×2 matrix

$$H=-i\hbar v_F\begin{pmatrix}0 & \partial/\partial x-i\partial/\partial y\\ \partial/\partial x+i\partial/\partial y & 0\end{pmatrix}. \tag{2}$$

Here, $\hbar$ is Planck's constant and v_F is the Fermi velocity (the single constant characterizing electrons in graphene), whose value is about 300 times smaller than that of light. The wave function has a two component structure (spinor)

$$\Psi(\mathbf{r},t)=\begin{pmatrix}u(\mathbf{r},t)\\ v(\mathbf{r},t)\end{pmatrix}. \tag{3}$$

The u and v components represent the electronic wavefunction in two graphene crystal sublattices. Equation (2) is often called the Dirac Hamiltonian in analogy to the Hamiltonian in the Dirac equation, which describes electrons and positrons in relativistic quantum mechanics.[8]

Because of the gapless spectrum (there is no energy gap between the electron and hole parts of the band), the exotic Klein effect is expected to take place.[9] The Klein effect for electrons and positrons was predicted more than half a century ago,[10] and its nature in the context of graphene is demonstrated in Fig. 3. Assume that an incident electron 1 coming from the left meets the electrical barrier as shown in Fig. 3. Due to conservation of energy, the electron moves along the horizontal dashed line. Classically, the electron, whose energy E is less than the potential of the barrier, cannot pass it and is always reflected. Quantum mechanically, an electron with a quadratic dispersion law can tunnel through the barrier. However, the tunneling probability decreases exponentially with the thickness of the barrier. The Dirac electron has another possibility and turns into hole 2 in the barrier.[11] At the end of the barrier, it changes back into electron 3 and continues its motion. For perpendicular incidence, the probability of such a process is unity and does not depend on the thickness of the barrier.

Measurements in graphene can also be done in bilayer graphene to emphasize the peculiar features of the electrons with a conic type spectrum. The spectrum of the low energy excitations in bilayer graphene is shown in Fig. 2(b). It consists of two paraboloids touching each other at their vertices.

The Klein effect takes place in bilayer graphene as well, because energy conservation does not preclude an electron from turning into a hole under the barrier. Nevertheless, quantum mechanical considerations show that the Klein ef-

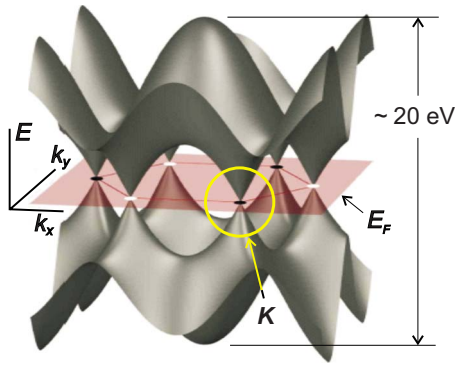

Fig. 1. (Color online) Conduction band in graphene.

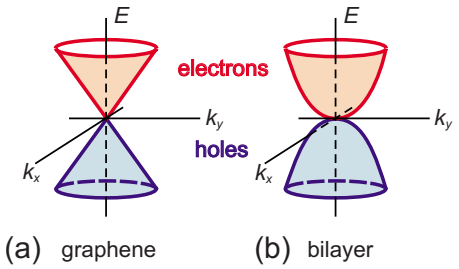

Fig. 2. (Color online) Electron and hole spectra in (a) graphene and (b) bilayer graphene in the vicinity of the K point.

fect in bilayer graphene is quite different. For instance, for perpendicular incidence, the probability for an electron to tunnel through the barrier is zero.

These exotic features of single and bilayer graphene are caused by the peculiarities of their lattices shown in Fig. 4. The graphene lattice is shown in Fig. 4(a). This lattice can be constructed by translating a primitive cell, which is shown by the shadowed parallelogram. One cell contains two carbon atoms (a solid circle and an open one). The conic point K in the graphene spectrum is a direct consequence of this primitive cell. The lattice of bilayer graphene is also seen in Fig. 4 and its top view is presented in Fig. 4(a). The upper layer coincides with that of graphene, and the lower one is slightly shifted aside. Figure 4(b) shows the side view of both layers. The most important property of this lattice, which determines its spectrum, is as follows. Only one sublattice (solid circles) of the upper layer has nearest neighbors in the lower layer, as indicated by dashed vertical lines in the side view [see Fig. 4(b)]. The interlayer distance c is about 36% larger than the lattice constant a, which enables the layers to be considered as weakly coupled.

The aim of this paper is to illustrate how the essential features of the spectra (the conic graphene and touching paraboloids for bilayer graphene) and the description of electrons and holes by the Dirac Hamiltonian result from the symmetry properties of the lattices. Simple one-dimensional (1D) models and the tight-binding approach are used for this purpose. These 1D models bridge nanophysics with the chemistry of conjugated polymers.[12]

The paper is organized as follows. In Sec. II we present aspects of the mathematical technique based on the tight-binding model and long-wavelength approximation and consider the spectrum of electrons in the simplest 1D model. In Sec. III a modified chain is presented whose spectrum is the analog of excitations in graphene. Section IV is devoted to the more sophisticated 1D model, which illustrates the spectrum of bilayer graphene. Our conclusions are given in Sec. V.

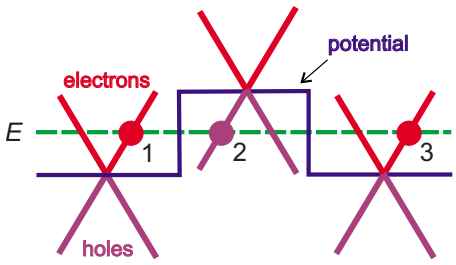

Fig. 3. (Color online) Klein effect in graphene.

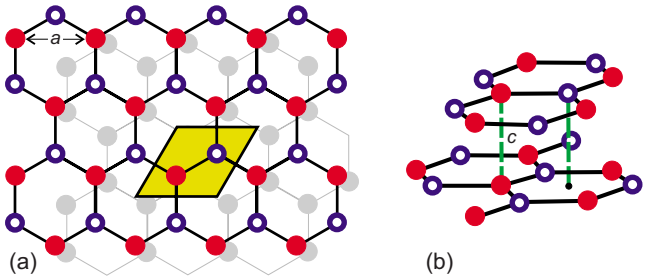

Fig. 4. (Color online) Lattice of single layer and bilayer graphene. (a) The graphene lattice; the shaded parallelogram indicates a primitive cell. The second bilayer graphene layer is shown in light grey; (b) side view of bilayer graphene lattice.

II. SIMPLE 1D LATTICE

We consider 1D electron systems described by the time dependent Schrödinger equation

$$i\hbar\frac{\partial}{\partial t}\Psi(t) = H\Psi(t) \tag{4}$$

and the stationary Schrödinger equation

$$(H - E)\Psi = 0, \tag{5}$$

where the eigenvalue E gives the single-electron energy.

A. Tight-binding model

Our main tool will be the tight-binding model and the long-wavelength approximation. We shall review the essential features of this tool by considering the simple 1D lattice shown in Fig. 5. This lattice is composed of atoms (solid circles) equidistantly spaced along the x axis, shown by the straight black line. It can be used as a model of electron motion along the carbon atoms in a polyethylene chain. We display a primitive cell (as a rectangle) containing a single atom and label cells by the integer n.

The tight-binding approach[13] (see also Refs. 14–16) is based on the idea that the atomic potential is deep and electron tunneling between the neighboring atoms is weak. In this approach, the electron is described by the complex amplitudes u_n such that $P_n = |u_n|^2$ gives the probability of finding the electron at site n. In the simplest version of the approach, these amplitudes satisfy the equation

$$i\hbar\frac{d}{dt}u_n = -W(u_{n-1} + u_{n+1}), \tag{6}$$

which is the tight-binding analogue of the Schrödinger equation (4). To simplify the notation, we shall use dimensionless units by measuring all distances in lattice constants a, energy in units related to the tunneling amplitude W, and the time in $\hbar/W$. These units enable us to rewrite Eq. (6) as

$$i\frac{d}{dt}u_n = Hu_n \equiv -(u_{n-1} + u_{n+1}). \tag{7}$$

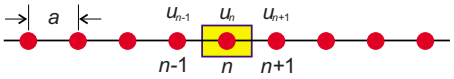

Fig. 5. (Color online) The simplest 1D lattice.

The analysis of discrete equations of this type is the principal technique used in this paper. The single-electron spectrum follows from the equation

$$Eu_n = Hu_n \equiv -(u_{n-1} + u_{n+1}) \tag{8}$$

which is the analogue of the eigenvalue problem in Eq. (5).

B. Translation symmetry

The discrete eigenvalue problem (8) can be solved in various ways. Because our main purpose is to discuss the relation between spectrum and symmetry, we introduce the translation operator T,

$$u_{n+1} = Tu_n, \tag{9}$$

which translates the lattice by unit length (the length of the primitive cell). The infinite lattice shown in Fig. 5 is invariant under the action of this operator. The translation operator enables us to rewrite Eqs. (7) and (8) in a more elegant form by expressing the Hamiltonian as

$$H = -(T^{-1} + T), \tag{10}$$

where T^{-1} is the inverse operator defined via $u_{n-1} = T^{-1}u_n$.

Now we can formulate the translation property as the zero commutator of the translation operator with the Hamiltonian:

$$[T,H] = TH - HT = 0, \tag{11}$$

which is obvious because the Hamiltonian (10) is composed of the same translation operators.

This formal manipulation is useful because the commuting operators can be characterized by the same eigenfunctions. The eigenfunctions of the Hamiltonian can be found by solving the eigenvalue problem for the translation operator T:

$$Tu_n = \lambda u_n, \tag{12}$$

which often is simpler than the original eigenvalue problem (8).

The difference Eqs. (8) and (12), like the analogous differential equations, need boundary conditions. We follow the standard procedure by replacing the infinite lattice with a finite length chain ($0 \leqslant n < N$) and applying periodic (Born–von Karman) boundary conditions

$$u_N = T^N u_0 = \lambda^N u_0 = u_0. \tag{13}$$

Thus, the algebraic equation $\lambda^N = 1$ has to be satisfied. It has complex eigenvalues

$$\lambda_m = \lambda_k = e^{ik}, \tag{14}$$

where

$$k = \frac{2\pi}{N} m, \quad (m = 0, \pm 1, \pm 2, \cdots). \tag{15}$$

For simplicity, we do not index the variable k, but remember that it is a discrete variable with the small $\Delta k = 2\pi/N$ distance between neighboring values, and it can be used for numbering the eigenvalues instead of the integer m. It is the wave vector (or quasi-momentum) of the electron.

The eigenfunctions of the translation operator can be constructed by means of the same T operator. By using Eq. (12) n times we obtain

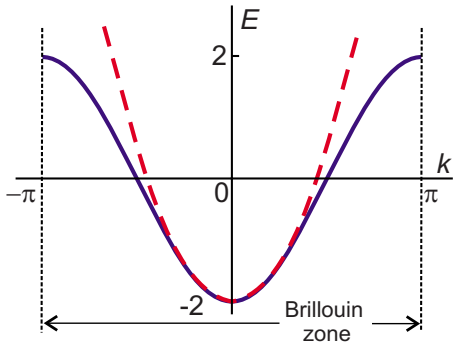

Fig. 6. (Color online) Electron spectrum in the simplest 1D lattice. The dashed curve is the long-wavelength approximation to this spectrum.

$$u_n = T^n u_0 = \lambda^n u_0 = e^{ikn} u_0. \tag{16}$$

Thus, to within a normalization constant, the eigenfunction of the T operator is

$$u_n = e^{ikn}. \tag{17}$$

C. Spectrum

As mentioned, the translation operator eigenfunctions coincide with those of the Hamiltonian. We substitute Eq. (17) into the Schrödinger equation (8) and obtain the following energy for the electron:

$$E \equiv \varepsilon(k) = -(e^{-ik} + e^{ik}) = -2\cos k. \tag{18}$$

This electron spectrum for the simplest 1D lattice is shown in Fig. 6 by the solid curve. It is a typical spectrum for the tight-binding model. The spectrum is a periodic function of the quasi-momentum k, as it is in any periodic lattice. In Fig. 6, the spectrum is shown in the interval $k = (-\pi, \pi)$, known as the first Brillouin zone.

D. Schrödinger equation and effective mass

We now consider the long-wavelength approximation, which is valid for excitations whose characteristic wavelength is much larger than the lattice constant, namely, when $k \ll 1$. The standard way of solving such problems is by replacing the difference tight-binding model equation by the differential one. Mathematically, the long-wavelength approximation is based on the expansion of all functions in a power series in k. For instance, if we use this approximation instead of Eq. (18) for the electron energy, we obtain the simpler expression

$$E \approx -2(1 - k^2/2) = -2 + k^2. \tag{19}$$

Thus, we obtain the standard parabolic band, which is shown in Fig. 6 by the dashed curve. If we replace the site label n with the continuous electron coordinate x, we may replace Eq. (7) with the differential equation

$$i\frac{\partial}{\partial t} u(x) = -[u(x-1) + u(x+1)]$$

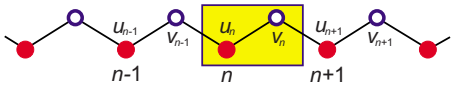

Fig. 7. (Color online) Corrugated 1D lattice.

$$\approx -\left\{2+\frac{\partial^2}{\partial x^2}\right\}u(x), \tag{20}$$

which is known as the Schrödinger equation in the effective mass approximation.[17] The effective mass can be obtained by going back to the original units, namely, $m^*=\hbar/2Wa^2$.

III. MODIFIED 1D LATTICE

To illustrate the electron spectrum in graphene, we consider a more sophisticated case, the corrugated lattice shown in Fig. 7.[18] This modified lattice differs from the one shown in Fig. 5 in several aspects. It is corrugated, that is, the atoms indicated by open circles are shifted up with respect to those indicated by solid circles. The new lattice contains two atoms in the primitive cell, as is shown in Fig. 7 by the shadowed rectangle. We assume that tunneling amplitudes along the tilted bonds are both the same. Thus, the problem is formally the same but with different notation u_n for the electron amplitude at the solid circle and the symbol v_n for the open circle. The Schrödinger equation (7) is replaced by two coupled equations:

$$i\frac{\partial}{\partial t}u_n=-(v_{n-1}+v_n), \tag{21a}$$

$$i\frac{\partial}{\partial t}v_n=-(u_n+u_{n+1}). \tag{21b}$$

A. Symmetry properties

By translational symmetry, the lattices in Secs. II and III are different, because the primitive cell is twice as large for the corrugated lattice. This lattice is no longer invariant under the action of the translation operator T but is invariant under translation by two sites or under the action of operator T_2, which is defined by

$$T_2u_n=u_{n+1},\quad T_2v_n=v_{n+1}. \tag{22}$$

For simplicity, we introduce a two-component wave function for the electron amplitudes:

$$\psi_n=\begin{pmatrix}u_n\\v_n\end{pmatrix}. \tag{23}$$

From now on, script symbols for the operators will be used to represent 2×2 matrices. Thus, instead of Eq. (22), we use the notation

$$\mathcal{T}_2\psi_n=\psi_{n+1},\quad \mathcal{T}_2=\begin{pmatrix}T_2&0\\0&T_2\end{pmatrix}. \tag{24}$$

Equation (21) can be represented as a Schrödinger equation with the matrix Hamiltonian:

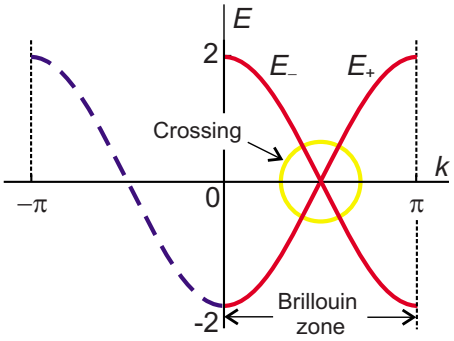

Fig. 8. (Color online) Electron spectrum for the corrugated 1D lattice.

$$\mathcal{H}=-\begin{pmatrix}0&1+T_2^{-1}\\1+T_2&0\end{pmatrix}. \tag{25}$$

It is straightforward to check that this Hamiltonian commutes with the translation operator $\mathcal{T}_2$, and consequently, its eigenfunctions can be obtained by solving the eigenvalue problem for $\mathcal{T}_2$. If we impose the modified Born–von Karmen boundary conditions $u_{N/2}=u_0$ and $v_{N/2}=v_0$ and use the same definition for k as in Eq. (15), we obtain the eigenvalues of the new translation operator $\lambda_m=\lambda_k=\exp(2ik)$ and its eigenfunctions:

$$\psi_n=e^{2ikn}\psi=e^{2ikn}\begin{pmatrix}u\\v\end{pmatrix}. \tag{26}$$

These eigenvalues do not solve the spectrum problem, because the translation operator $\mathcal{T}_2$ is weaker (it has half as many eigenvalues as the operator T). Consequently, the eigenfunction (26) has two undetermined constants (u,v). We substitute this eigenfunction into Eq. (5) and obtain two algebraic equations

$$Eu=-(e^{-2ik}+1)v=-e^{-ik}\varepsilon(k)v, \tag{27a}$$

$$Ev=-(1+e^{2ik})u=-e^{ik}\varepsilon(k)u. \tag{27b}$$

We set to zero the determinant of Eq. (27) and obtain the dispersion relation

$$E^2=\varepsilon^2(k) \tag{28}$$

where $\varepsilon(k)$ is given by Eq. (18), so that the spectrum becomes

$$E=E_\pm=\pm\varepsilon(k), \tag{29}$$

which is shown in Fig. 8 by two solid curves.

We see that the spectrum is the same as for the simpler lattice considered in Sec. II C, shown in Fig. 8 by a dashed curve, but is interpreted differently. The left part of the spectrum branch from the simpler lattice has been translated to the right by the shortest reciprocal lattice vector $(2\pi/2)$ of the corrugated lattice to fit it in the Brillouin zone (which is smaller by a factor of two). There are two spectrum branches because there are two single level atoms in the primitive cell.

Figure 8 shows the crossing of two spectrum branches, which is possible only for branches with different symmetry properties. We next discuss what kind of symmetry allows these branches to cross each other.

B. Combined symmetry

From Fig. 7 it is easy to find one more symmetry operation under which the corrugated lattice is invariant. It is the translation of the lattice by unity (by half of the primitive cell length), followed by a reflection in the transverse direction ($u \leftrightarrows v$). It is the analogue of the glide plane known in 3D lattices.[19] This combined operation can be represented by the operator

$$\mathcal{K} = \begin{pmatrix} 0 & T^{-1} \\ T & 0 \end{pmatrix}, \tag{30}$$

where this T operator translates the lattice by unity (by half of the primitive cell) and is defined as

$$Tu_n = u_{n+1/2}, \quad Tv_n = v_{n+1/2}. \tag{31}$$

It follows from Eq. (31) that $T^2 = T_2$, and $\exp(ik)$ is the eigenvalue of the operator T, corresponding to the eigenfunction (26). A straightforward calculation confirms that the operator $\mathcal{K}$ commutes with the Hamiltonian (25), and consequently the equation

$$\mathcal{K}\psi = \kappa\psi \tag{32}$$

can be used to classify the electron spectrum branches. The eigenvalues and corresponding eigenfunctions are

$$\kappa_+ = 1, \quad \psi_n^{(+)} = e^{2ikn}\begin{pmatrix} 1 \\ e^{ik} \end{pmatrix}, \tag{33a}$$

$$\kappa_- = -1, \quad \psi_n^{(-)} = e^{2ikn}\begin{pmatrix} 1 \\ -e^{-ik} \end{pmatrix}. \tag{33b}$$

If we substitute these eigenfunctions into Eq. (27), we find that the sign of the energy in Eq. (29) coincides with the sign of the eigenvalue $\kappa_\pm$.

We now see that the two spectrum branches shown in Fig. 8 by solid curves are differentiated by a new quantum number κ. Consequently, they have different symmetry, and their crossing does not contradict quantum mechanics. For the two-dimensional graphene lattice, this quantum number is known as *chirality*.[20]

C. Dirac Hamiltonian

The crossing of spectrum branches in Fig. 8 is the 1D analogue of the K point in the two-dimensional graphene spectrum shown in Fig. 2(a). We now assume that the Fermi energy coincides with the intersection point (as in graphene and conjugated polymer polyacetylene), and we focus on the excitations close to it and exploit the long-wavelength approximation. Namely, we change the origin of the Brillouin zone by the substitution

$$k \to \frac{\pi}{2} + k, \tag{34}$$

and consider the small momentum limit ($k \ll 1$). After this replacement, the electron spectrum (29) becomes

$$E_\pm = \mp 2\cos(k + \pi/2) = \pm 2\sin k \approx \pm 2k, \tag{35}$$

which resembles the conic spectrum of two-dimensional graphene. In this long-wavelength approximation, the Hamiltonian (25) has to be changed as follows:

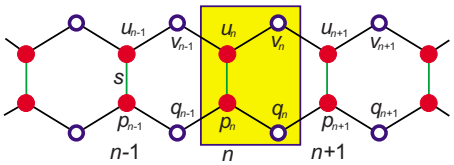

Fig. 9. (Color online) Twofold corrugated 1D lattice.

$$\mathcal{H} = -\begin{pmatrix} 0 & 1 + e^{-2i(\pi/2+k)} \\ 1 + e^{2i(\pi/2+k)} & 0 \end{pmatrix} = -\begin{pmatrix} 0 & 1 - e^{-2ik} \\ 1 - e^{2ik} & 0 \end{pmatrix} \approx -2\begin{pmatrix} 0 & ik \\ -ik & 0 \end{pmatrix}. \tag{36}$$

This Hamiltonian acts on the wave function (26). To generalize it for any wave function, we have to replace the momentum k by its differential analogue $-id/dx$, which converts the Hamiltonian to

$$\mathcal{H} = 2\begin{pmatrix} 0 & -d/dx \\ d/dx & 0 \end{pmatrix}. \tag{37}$$

Equation (37) is the 1D analogue of the Dirac Hamiltonian (2) used in the description of electrons and holes in graphene.

IV. TWOFOLD CORRUGATED 1D LATTICE

We now discuss a more complicated lattice that will serve as an analogue for charge carriers in bilayer graphene. It is composed of two corrugated 1D chains[21] as shown in Fig. 9. In this lattice, electrons can tunnel along the chain (with the amplitude equal to unity), as in the lattices we have considered previously, and also jump to the neighboring chain. This transverse tunneling (shown by vertical lines) is possible only between the closest neighboring sites (solid circles), because it is the analogue of the bilayer graphene lattice shown in Fig. 4. We assume that this weak tunneling between the chains is characterized by a dimensionless tunneling amplitude s.

A. Schrödinger equation and translation symmetry

In the primitive cell (shown by the rectangle), there are four atoms. We generalize the description in Sec. III A and use a four-component wave function (a collection of the electron amplitudes on the different sites indicated in Fig. 9)

$$\psi_n = \begin{pmatrix} u_n \\ v_n \\ p_n \\ q_n \end{pmatrix}. \tag{38}$$

This lattice is invariant under the action of the translation operator $\psi_{n+1} = T_2\psi_n$, from which it follows that the wave function can be represented as

$$\psi_n = T_2^n \psi = e^{2ikn} \begin{pmatrix} u \\ v \\ p \\ q \end{pmatrix}. \tag{39}$$

The wave function satisfies the stationary Schrödinger equation (5) [or Eq. (4)] with the 4×4 matrix Hamiltonian:

$$\mathcal{H} = -\begin{pmatrix} 0 & 1+T_2^{-1} & s & 0 \\ 1+T_2 & 0 & 0 & 0 \\ s & 0 & 0 & 1+T_2^{-1} \\ 0 & 0 & 1+T_2 & 0 \end{pmatrix}. \tag{40}$$

B. Additional symmetry and spectrum

If we substitute the wave function (39) into the stationary Schrödinger equation with the Hamiltonian in Eq. (40), we obtain four linear equations for the wave function components u, v, p, and q. To simplify the calculation, we notice that the lattice has an additional symmetry: it is invariant under a reflection in the transverse direction, which can be represented with the aid of the operator P defined by

$$Pu = p, \quad Pp = u, \quad Pv = q, \quad Pq = v. \tag{41}$$

The inversion applied twice is equivalent to the identity operation ($P^2=1$), and thus the eigenvalues of the operator P are equal to $\xi_\pm = \pm 1$. It can be considered as the parity operator, and hence the eigenfunctions of P are the analogues of the symmetric and antisymmetric functions, namely,

$$\xi_\pm = \pm 1: \quad U_\pm = u \pm p, \quad V_\pm = v \pm q. \tag{42}$$

We introduce symmetric and antisymmetric eigenfunctions

$$\psi_n^{(\pm)} = e^{2ikn} \begin{pmatrix} U_\pm \\ V_\pm \\ \pm U_\pm \\ \pm V_\pm \end{pmatrix}, \tag{43}$$

substitute them into the stationary Schrödinger equation, and obtain two decoupled equation ($\pm$)-sets:

$$(E^{(\pm)} \mp s) U_\pm = -\varepsilon(k) V_\pm, \tag{44a}$$

$$E^{(\pm)} V_\pm = -\varepsilon(k) U_\pm. \tag{44b}$$

Their solution leads to the following spectra for two noninteracting electron systems:

$$E_\pm^{(+)} = \frac{s}{2} \pm \sqrt{\varepsilon^2(k) + s^2/4}, \tag{45a}$$

$$E_\pm^{(-)} = -\frac{s}{2} \pm \sqrt{\varepsilon^2(k) + s^2/4}. \tag{45b}$$

This spectrum is shown in Fig. 10 in the small Brillouin zone (as in the previous case of a single corrugated chain spectrum). The noninteracting groups of spectrum branches are shown by solid and dashed lines. These spectrum branches have different symmetry, and the corresponding eigenfunctions differ by their parity with respect to inversion along the transverse direction. The spectrum branches in each group (solid or dashed) have the same symmetry, which is why they repel each other, and we see an *anticrossing*. The model

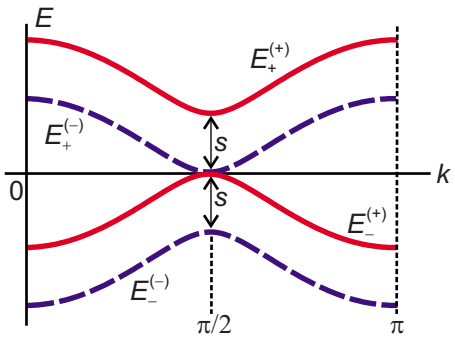

Fig. 10. (Color online) Electron spectrum in a twofold corrugated lattice.

is characterized by a single constant s that is responsible for the energy gaps in the groups and the shift between the groups as well. That is why we see the touching branches at the point $k=\pi/2$ for any value of the parameter s.

C. Dirac Hamiltonian

We focus on the analogue of bilayer graphene and 1D polymer acene and assume that the Fermi energy coincides with the touching point of the two spectrum branches in Fig. 10. Let us consider the long-wavelength approximation and move the zero point of the k-axis to the touching point by means of transformation (34), and let us assume that the new quasi-momentum satisfies the condition $k \ll 1$. In this case, the expansion of the Hamiltonian (40) in a power series in k converts it into

$$\mathcal{H} = 2\begin{pmatrix} 0 & -ik & -s/2 & 0 \\ ik & 0 & 0 & 0 \\ -s/2 & 0 & 0 & -ik \\ 0 & 0 & ik & 0 \end{pmatrix}. \tag{46}$$

By changing the momentum k to the corresponding derivative $-id/dx$ [as was done in Eq. (37)], we arrive at the 4×4 matrix Hamiltonian:

$$\mathcal{H} = 2\begin{pmatrix} 0 & -d/dx & -s/2 & 0 \\ d/dx & 0 & 0 & 0 \\ -s/2 & 0 & 0 & -d/dx \\ 0 & 0 & d/dx & 0 \end{pmatrix} \tag{47}$$

which is valid in the long-wavelength approximation. This matrix is the 1D analogue of the two-dimensional Dirac Hamiltonian used to describe the electrons and holes in bilayer graphene.

D. Two-band approximation

If we are interested only in electrons and holes with excitation energies much less than the energy gap (whose value coincides with the value of parameter s, see Fig. 10 a further simplification is possible. In this case, only two central branches in the spectrum shown in Fig. 10 are important. We construct such a two-band approximation and start from Eq. (4) with the Hamiltonian (47) and rewrite it as the following set of equations for the wave function components:

$$i\frac{\partial}{\partial t}u = -\frac{\partial}{\partial x}v + \frac{s}{2}p, \tag{48a}$$

$$i\frac{\partial}{\partial t}v = \frac{\partial}{\partial x}u, \tag{48b}$$

$$i\frac{\partial}{\partial t}p = -\frac{\partial}{\partial x}q + \frac{s}{2}u, \tag{48c}$$

$$i\frac{\partial}{\partial t}q = \frac{\partial}{\partial x}p. \tag{48d}$$

Next, we assume that the variations of wave function components in time and in space are small, namely,

$$\partial/\partial x \sim k \ll s, \quad \partial/\partial t \sim \varepsilon \sim k^2/s \ll s. \tag{49}$$

It follows from Eqs. (48b) and (48d) that the wave function components u and p are much smaller than the components v and q, which enables us to neglect the left-hand side terms in Eqs. (48a) and (48c). Thus, the small components are obtained from Eqs. (48a) and (48c)

$$u = \frac{2}{s}\frac{\partial}{\partial x}q, \quad p = \frac{2}{s}\frac{\partial}{\partial x}v. \tag{50}$$

We substitute them into Eqs. (48b) and (48d) and obtain

$$i\frac{\partial}{\partial t}v = \frac{4}{s}\frac{\partial^2}{\partial x^2}q, \quad i\frac{\partial}{\partial t}q = \frac{4}{s}\frac{\partial^2}{\partial x^2}v, \tag{51}$$

which can be rewritten as a standard Schrödinger equation for the two-component wave function

$$\psi = \begin{pmatrix} v \\ q \end{pmatrix}, \tag{52}$$

with the following 2×2 matrix Hamiltonian:

$$\mathcal{H} = \frac{4}{s}\begin{pmatrix} 0 & \partial^2/\partial x^2 \\ \partial^2/\partial x^2 & 0 \end{pmatrix}, \tag{53}$$

which is the 1D analogue of the two-dimensional Hamiltonian used for the description of electrons and holes in bilayer graphene in the two-band approximation.

V. CONCLUSIONS

We have shown that the peculiarities of the excitation spectra in single and bilayer graphene, namely, the conic type spectrum at the K-point in graphene and the touching of different symmetry spectrum branches in bilayer graphene, have analogies in the electron spectrum in 1D chains and are mainly caused by translation and additional symmetries. Such analogies can be useful pedagogically and can motivate us to look for similar electronic phenomena in two-dimensional graphene and 1D polymers. For instance, the Klein effect should also occur in *trans*-polyacetylene.

ACKNOWLEDGMENTS

The authors would like to acknowledge the referees for their thoughtful and stimulating comments. We thank Professor R. Katilius for helpful discussions. This work was supported by the Flemish Science Foundation (FWO-Vl) and the Belgian Science Policy (IAP).

[a]Electronic mail: amatulis@takas.lt
[b]Electronic mail: francois.peeters@ua.ac.be

[1] H. W. Kroto, J. R. Heath, S. C. O'Brien, R. F. Curl, and R. E. Smalley, "C60: Buckminsterfullerene," Nature (London) **318**, 162–163 (1985).
[2] S. Iijima and T. Ichihashi, "Single-shell carbon nanotubes of 1 nm diameter," Nature (London) **363**, 603–605 (1993).
[3] K. S. Novoselov, A. K. Geim, S. V. Morozov, D. Jiang, Y. Zhang, S. V. Dubouos, I. V. Grigorjeva, and A. A. Firsov, "Electric field effect in atomically thin carbon films," Science **306**, 666–669 (2004).
[4] J. C. Meyer, A. K. Geim, M. I. Katsnelson, K. S. Novoselov, T. J. Booth, and S. Roth, "The structure of suspended graphene sheets," Nature (London) **446**, 60–63 (2007).
[5] A. K. Geim and P. Kim, "Carbon wonderland," Sci. Am. (Int. Ed.) **298**(4), 90–97 (2008).
[6] A. K. Geim and K. S. Novoselov, "The rise of graphene," Nature Mater. **6**, 183–191 (2007).
[7] M. Wilson, "Electrons in atomically thin carbon sheets behave like massless particles," Phys. Today **59**, 21–23 (2006).
[8] P. A. M. Dirac, "The quantum theory of the electron," Proc. R. Soc. London, Ser. A **117**, 610–624 (1928); "The quantum theory of the electron, part II," **118**, 351–361 (1928).
[9] M. I. Katsnelson, K. S. Novoselov, and A. K. Geim, "Chiral tunneling and the Klein paradox in graphene," Nat. Phys. **2**, 620–625 (2006).
[10] O. Klein, "Die reflexion von elektronen an einem potentialsprung nach der relativischen dynamik von Dirac," Z. Phys. **53**, 157–165 (1929).
[11] Tunneling in graphene is actually a complicated many-particle process. Due to charge conservation, the hole and electron move in opposite directions. Thus, the electron–hole pair is generated at the end of the barrier, and the hole annihilates with the incoming electron.
[12] L. Malysheva and A. Onipko, "From acene to graphene spectrum of π electrons with the use of the Green's function," Phys. Status Solidi C **245**, 2132–2136 (2008).
[13] F. Bloch, "Über die Quantenmechanik der Elektronen in Kristallgittern," Z. Phys. **52**, 555–600 (1928).
[14] J. C. Slater and G. F. Koster, "Simplified LCAO method for the periodic potential problem," Phys. Rev. **94**, 1498–1524 (1954).
[15] N. W. Ashcroft and N. D. Mermin, *Solid State Physics* (Saunders College Publishing, Fort Worth, 1976), Sec. 10.
[16] A. Šiber, "Dynamics and (de)localization in a one-dimensional tight-binding chain," Am. J. Phys. **74**(8), 692–698 (2006).
[17] A. O. E. Animalu, *Intermediate Quantum Theory of Crystalline Solids* (Prentice Hall, Englewood Cliffs, NJ, 1977), Chap. 5, Sec. 7.
[18] This 1D lattice can be considered as a simple model of the trans-polyacetylene chain. See A. J. Heeger, S. Kivelson, J. R. Schrieffer, and W.-P. Su, "Solitons in conducting polymers," Rev. Mod. Phys. **60**, 781–850 (1988).
[19] N. W. Ashcroft and N. D. Mermin, *Solid State Physics* (Saunders College Publishing, Fort Worth, 1976), Sec. 7.
[20] F. D. M. Haldane, "Model for a quantum Hall effect without Landau levels: Condensed-matter realization of the 'Parity anomaly'," Phys. Rev. Lett. **61**, 2015–2018 (1988).
[21] In the chemistry of polymers such 1D lattice corresponds to acene (Ref. 12).